

Molecular Assemblies Containing Linear and Bent [Fe^{III}–CN–Cu^{II}] Bridge Units: Synthesis, Structures, and Relevance to Cyanide-Inhibited Heme–Copper Oxidases

Michael J. Scott and R. H. Holm*

Contribution from the Department of Chemistry, Harvard University, Cambridge, Massachusetts 02138

Received July 14, 1994[⊗]

Abstract: A series of molecular complexes containing the [Fe^{III}–CN–Cu^{II}] bridge unit has been prepared and structurally characterized as a means of establishing the presence of a similar bridge in cyanide-inhibited cytochrome *c* oxidase and terminal quinol oxidases. The series consists of the molecules [(py)(OEP)Fe–CN–Cu(L/L')]^{2+/+} with L/L' = Me₅dien/Me₂CO (**11**) and bnpy₂/OTf (**12**), and L = TIM (**13**), cyclops (**14**), and cyclam (**15**). These species were prepared by the reaction of [Fe(OEP)(py)(CN)] (**1**) with the appropriate Cu(II) precursors in acetone or acetonitrile/dichloromethane solutions. Because Cu_B sites in enzymes are structurally undefined, the stereochemistry of these precursors was varied. When combined with the previously reported species L = Me₆tren (**9**) and L/L' = Me₅dien/OTf (**10**), they constitute a set of seven monobridged species. Also prepared was {[py)(OEP)Fe(CN)]₂Cu(cyclam)}²⁺ (**16**), shown to contain the [Fe^{III}–CN–Cu^{II}–NC–Fe^{III}] bridge, and [(OEP)Fe–NC–Cu(Me₅dien)]⁺ (**17**). The X-ray structures of precursor complexes [Cu(Me₅dien)(OH₂)(OCMe₂)]²⁺, [Cu(bnpy₂)(OTf)₂], [Cu(cyclam)(MeCN)₂]²⁺, and [Cu(Me₅dien)(MeCN)]⁺ and the bridged assemblies **11–14**, **16**, and **17** were determined; those of **9** and **10** have been described earlier. The structures of the heme and Cu(II) fragments differ little from those of **1** and the Cu(II) starting compounds, respectively. In all bridges, the Fe^{III}–CN fragment is linear (bond angle 176–180°) and any deviations therefrom occur in the Cu^{II}–CN fragment. Nearly linear bridges occur in **9** (trigonal bipyramidal-ax) and **10/11** (distorted square pyramidal-eq) (Cu–N–C = 170–174°). Bent bridges are found in **12** (163°, distorted square pyramidal-eq), and in **13** (147°) and **14** (159°) (both square pyramidal-ax). The smallest angle is observed in doubly bridged **16** (140°, tetragonal octahedral). In the bridges, decreasing Cu–N–C bond angles correlate with increasing Cu–NC bond distances. Cyanide stretching frequencies in the crystalline state and in dichloromethane solution are nearly the same and in the solids cover the interval 2181–2120 cm⁻¹; nearly all values exceed that of **1** (2129 cm⁻¹). Increasing ν_{CN} values correlate with decreasing Cu–N–C angles and increasing Cu–N bond distances. These values encompass those for cyanide-inhibited oxidized enzymes (2152–2146 cm⁻¹). The infrared data, together with magnetic and Mössbauer spectroscopic results which show coupled Fe(III) and Cu(II) spins, lead to the conclusion that these enzymes possess a tight [Fe^{III}–CN–Cu^{II}] bridge, rather than a binuclear site in which cyanide is bridged exclusively to one subsite, or interacts weakly with another subsite, or is hydrogen-bonded at the uncoordinated end. The existence of the [Fe^{III}–NC–Cu^I] bridge in **17** raises the matter of a similar atom sequence in biological bridges of the same oxidation state. (bnpy₂ = *N,N*-bis(2-(2-pyridylethyl))benzylamine, Me₅dien = 1,1,4,7,7-pentamethyldiethylenetriamine, Me₆tren = tris(2-(dimethylamino)ethyl)amine, OEP = octaethylporphyrinate(2-), OTf = CF₃SO₃⁻, py = pyridine; cyclops, TIM, cyclam = tetraazamacrocycles; ax = axial, eq = equatorial, referring to the position of cyanide substitution in the Cu(II) coordination sphere.)

Introduction

We are engaged in the continuing development of the chemistry of bridged binuclear iron–copper systems relevant to the iron–copper (heme *a*₃/Cu_B) binuclear site of eukaryotic cytochrome *c* oxidases and prokaryotic cytochrome and quinol oxidases.¹ In the oxidized (“as-isolated”) state of the enzymes, this site is composed of a high-spin Fe(III) heme axially coordinated to an imidazole ligand distal to a Cu(II) atom that is minimally coordinated by three imidazole groups. The stereochemistry at the Cu_B subsite is unestablished. The metal centers are antiferromagnetically coupled through a bridging atom to generate an *S* = 2 ground state. The most recent structural results for a binuclear site pertain to that in the quinol-oxidizing cytochrome *aa*₃ from *Bacillus subtilis*. The Fe and

Cu EXAFS have been analyzed in terms of a S or Cl ligand asymmetrically bridging the two metals separated by 3.70 Å.² Current evidence suggests that the essential features of the binuclear site are largely conserved over the many enzymes that constitute the superfamily of heme–Cu oxidases.¹ When bridged, this site is one example of what we have termed bridged biological metal assemblies, in which two discrete fragments are juxtaposed wholly or in part by one or more covalent bridges.^{3,4} Our initial work on Fe–Cu bridged assemblies has resulted in the preparation and characterization of [(OEP)Fe–O–Cu(Me₆tren)]⁺,⁵ the first proven example of the [Fe^{III}–O–Cu^{II}] bridge unit.^{6,7} This species displays an *S* = 2 ground state but without apparent benefit of the bridge atom in *B. subtilis* cytochrome *aa*₃ or presumably other oxidases.

[⊗] Abstract published in *Advance ACS Abstracts*, November 15, 1994.

(1) (a) Saratse, M. *Q. Rev. Biophys.* **1990**, *23*, 331. (b) Babcock, G. T.; Wikström, M. *Nature* **1992**, *356*, 301. (c) Chan, S. I.; Li, P. M. *Biochemistry* **1990**, *29*, 1. (d) Malmström, B. *Chem. Rev.* **1990**, *90*, 1247; *Acc. Chem. Res.* **1993**, *26*, 332.

(2) Powers, L.; Lauraeus, M.; Reddy, K. S.; Chance, B.; Wikström, M. *Biochim. Biophys. Acta* **1994**, *1183*, 504.

(3) (a) Cai, L.; Weigel, J. A.; Holm, R. H. *J. Am. Chem. Soc.* **1993**, *115*, 9289. (b) Cai, L.; Holm, R. H. *J. Am. Chem. Soc.* **1994**, *116*, 7177.

(4) Holm, R. H. *Pure Appl. Chem.*, in press.

Oxidized and reduced heme-Cu oxidases bind a number of exogenous anions, among them cyanide.⁸⁻¹⁷ Binding of cyanide converts oxidized heme a_3 to a low-spin configuration, modifies magnetic coupling between Fe(III) and Cu(II), and otherwise influences all electronic properties of the site. Additionally, cyanide is an irreversible inhibitor of the oxidases, and its toxicity has been traced to binding to cytochrome *c* oxidase.¹⁸ Specifically, binding at the binuclear site would block uptake of dioxygen and suppress the reaction $O_2 + 4H^+ + 4e^- \rightarrow 2H_2O$, which is the final step in aerobic metabolism. The view that cyanide insinuates itself in the binuclear site in the inhibited form of the enzyme is encountered frequently in the oxidase literature. Most recently, when considering bound cyanide stretching frequencies, Palmer¹⁵ raised the issue of how cyanide binds in the binuclear site. In the oxidized enzyme, the possibilities are (i) a tight $[Fe^{III}-CN-Cu^{II}]$ bridge linear or somewhat bent, (ii) exclusive binding to one metal subsite, and (iii) tight binding at one subsite with the end atom weakly interacting either with the other subsite or with a proton in a hydrogen bond.

We have recently reported the first structurally authenticated examples of a heme-based $[Fe^{III}-CN-Cu^{II}]$ bridge unit.^{19,20} These occur in the assemblies $[(py)(OEP)Fe-CN-Cu(Me_6-tren)]^{2+}$ (**9**)²¹ and $[(py)(OEP)Fe-CN-Cu(Me_5dien)(OSO_2CF_3)]^+$ (**10**),²² which are schematically depicted in Figure 1. Because the structure of the Cu subsite in the binuclear enzyme site is unknown, the stereochemistry of the Cu fragment was varied from trigonal bipyramidal (TBP) in **9** to distorted square pyramidal (d-SP) in **10**, with the nitrogen end of cyanide coordinated in an equatorial position. Species **9** and **10** display

(5) Ligand abbreviations: bnpy₂, *N,N*-bis(2-(2-pyridylethyl))benzylamine; cyclam, 1,4,8,11-tetraazacyclotetradecane; cyclops, difluoro(3,3'-(trimethylenedinitrilo)bis(2-butanone oximate))borate(1-); HIm, imidazole; 1-Melm, 1-methylimidazole; Me₅dien, 1,1,4,7,7-pentamethyldiethylenetriamine; Me₆-tren, tris(2-(dimethylamino)ethyl)amine; OEP, octaethylporphyrinate(2-); py, pyridine; TIM, 2,3,9,10-tetramethyl-1,4,8,11-tetraazacyclotetradeca-1,3,8,10-tetraene.

(6) Lee, S. C.; Holm, R. H. *J. Am. Chem. Soc.* **1993**, *115*, 5833, 11789.

(7) This bridge type has since been reported by others: (a) Nanthakumar, A.; Fox, S.; Murthy, N. N.; Karlin, K. D.; Ravi, N.; Huynh, B. H.; Orosz, R. D.; Day, E. P.; Hagen, K. S.; Blackburn, N. *J. Am. Chem. Soc.* **1993**, *115*, 8513. (b) Karlin, K. D.; Nanthakumar, A.; Fox, S.; Murthy, N. N.; Ravi, N.; Huynh, B. H.; Orosz, R. D.; Day, E. P. *J. Am. Chem. Soc.* **1994**, *116*, 4753.

(8) Baker, G. M.; Noguchi, M.; Palmer, G. *J. Biol. Chem.* **1987**, *262*, 595.

(9) Yoshikawa, S.; Caughey, W. S. *J. Biol. Chem.* **1990**, *265*, 7945.

(10) Surerus, K. K.; Oerling, W. A.; Fan, C.; Gurbel, R. J.; Einarssdóttir, O.; Antholine, W. E.; Dyer, R. B.; Hoffman, B. M.; Woodruff, W. H.; Fee, J. A. *Proc. Natl. Acad. Sci. U.S.A.* **1992**, *89*, 3195.

(11) Caughey, W. S.; Dong, A.; Sanipath, V.; Yoshikawa, S.; Zhao, X.-J. *J. Bioenerg. Biomembr.* **1993**, *25*, 81.

(12) Tsubaki, M.; Yoshikawa, S. *Biochemistry* **1993**, *32*, 164.

(13) Li, W.; Palmer, G. *Biochemistry* **1993**, *32*, 1833.

(14) Tsubaki, M.; Mogi, T.; Anraku, Y.; Hori, H. *Biochemistry* **1993**, *32*, 6065.

(15) Palmer, G. *J. Bioenerg. Biomembr.* **1993**, *25*, 145.

(16) (a) Eglinton, D. G.; Johnson, M. K.; Thomson, A. J.; Gooding, P. E.; Greenwood, C. *Biochem. J.* **1980**, *191*, 319. (b) Thomson, A. J.; Johnson, M. K.; Greenwood, C.; Gooding, P. E. *Biochem. J.* **1981**, *193*, 687.

(17) (a) Kent, T. A.; Münck, E.; Dunham, W. R.; Filter, W. F.; Findling, K. L.; Yoshida, T.; Fee, J. A. *J. Biol. Chem.* **1982**, *257*, 12489. (b) Kent, T. A.; Young, L. J.; Palmer, G.; Fee, J. A.; Münck, E. *J. Biol. Chem.* **1983**, *258*, 8543.

(18) Lablanca, D. A. *J. Chem. Educ.* **1979**, *56*, 788. This article provides a brief account of and references to cyanide poisoning.

(19) This bridge has been demonstrated in largely polymeric compounds formed from Cu(II), dien, and $[Fe(CN)_6]^{3-4-}$: Morpurgo, G. O.; Mosini, V.; Porta, P.; Dessy, G.; Fares, V. *J. Chem. Soc., Dalton Trans.* **1980**, 1272; **1981**, 111.

(20) A similar heme-based bridge has apparently been prepared, but without X-ray structure proof: Gunter, M. J.; Berry, K. J.; Murray, K. S. *J. Am. Chem. Soc.* **1984**, *106*, 4227.

(21) Lee, S. C.; Scott, M. J.; Kauffmann, K.; Münck, E.; Holm, R. H. *J. Am. Chem. Soc.* **1994**, *116*, 401.

(22) Scott, M. J.; Lee, S. C.; Holm, R. H. *Inorg. Chem.* **1994**, *33*, 4651.

low-spin heme stereochemistry, nearly linear bridges, and slightly different ν_{CN} values. Cyanide stretching frequencies are not necessarily the most sensitive or informative reporters of structural differences. However, the observation that $\nu_{CN} = 2146-2152\text{ cm}^{-1}$ (aqueous buffer) for two different oxidases^{9,11-15} is substantially lower than $\nu_{CN} = 2174-2183\text{ cm}^{-1}$ (solid, solution) for **9**, **10**, and a closely related species²² necessitates a broader examination of the interplay of structures and stretching frequencies in $[Fe^{III}-CN-Cu^{II}]$ bridges. We report here the synthesis, structural characterization, and ν_{CN} data for some six new bridged species. These results, together with others from magnetic studies and Mössbauer, resonance Raman, and MCD spectroscopies, are directed toward elucidation of the geometric and electronic structures of the binuclear site in cyanide-inhibited oxidases. Some of the compounds reported have been used to augment the range of structures currently being investigated by these techniques. The results of these investigations will be described elsewhere.

Experimental Section⁵

Preparation of Compounds. All operations were conducted under a pure dinitrogen atmosphere using standard glovebox and Schlenk techniques. Solvents were dried according to standard procedures and were degassed prior to use.

(a) **Cu(II,I) Complexes.** $[Cu(Me_5dien)(OH_2)](ClO_4)_2$. A solution of 0.468 g (2.70 mmol) of Me₅dien in 5 mL of acetone was added dropwise to a solution of 1 g (2.70 mmol) of $[Cu(OH_2)_6](ClO_4)_2$ in 15 mL of acetone. The dark blue solution was stirred for 2 h and filtered; several volume equivalents of ether were diffused into the filtrate over 48 h, resulting in the formation of a dark blue crystalline mass. This material was collected and washed with THF and ether and dried to give the product as 1.02 g (83%) of a blue crystalline solid. Anal. Calcd for C₉H₂₅Cl₂CuN₃O₉: C, 23.83; H, 5.55; Cu, 14.01; N, 9.26. Found: C, 23.86; H, 5.48; Cu, 13.91; N, 9.18. When this material was crystallized from acetone/ether for X-ray diffraction purposes, the product was demonstrated to be $[Cu(Me_5dien)(OH_2)(OCMe_2)](ClO_4)_2 \cdot H_2O$ by a structure determination (vide infra).

$[Cu(bnpy_2)(OSO_2CF_3)_2]$. A solution of 0.479 g (6.35 mmol) of bnpy₂^{23,24} in 1 mL of acetone was added dropwise to a solution of 0.547 g (6.33 mmol) of $Cu(CF_3SO_3)_2$ in 10 mL of acetone. The dark bluesolution was stirred for 2 h; all volatiles were removed in vacuo. The solid residue was washed with THF and redissolved in 10 mL of acetone, and the solution was filtered. Several volume equivalents of ether were diffused into the filtrate over 24 h, resulting in the formation of a dark blue crystalline mass. The solid was collected and washed with THF and ether to yield 2.43 g (80%) of product as dark blue crystals. Anal. Calcd for C₂₃H₂₄CuF₆N₃O₆S₂: C, 40.68; H, 3.41; Cu, 9.36; N, 6.19. Found: C, 40.78; H, 3.35; Cu, 9.46; N, 6.14.

$[Cu(cyclam)](CF_3SO_3)_2$. A mixture of 0.415 g (2.07 mmol) of cyclam and 0.75 g (2.07 mmol) of $Cu(CF_3SO_3)_2$ was treated with 15 mL of methanol/acetonitrile (1:1 v/v). The reaction mixture was stirred for 2 h and filtered; the filtrate was reduced to dryness in vacuo. The solid residue was redissolved in a minimum amount of acetonitrile, and the solution was filtered; several volume equivalents of ether were diffused into the filtrate over 24 h. The solid was collected, washed with ether, and dried to afford the product as 0.99 g (85%) of red crystals. Anal. Calcd for C₁₂H₂₄CuF₆N₄O₆S₂: C, 25.65; H, 4.30; Cu, 11.31; N, 9.97. Found: C, 25.71; H, 4.34; Cu, 11.35; N, 9.96.

$[Cu(Me_5dien)(MeCN)](ClO_4)$. A solution of 0.483 g (2.79 mmol) of Me₅dien in 5 mL of acetonitrile was added dropwise to a solution of 0.913 g (2.79 mmol) of $[Cu(MeCN)_4](ClO_4)_2$ in 5 mL of acetonitrile. The solution was stirred for 2 h, and all volatiles were removed in vacuo. The solid residue was collected and washed with ether to yield 0.983 g (93%) of product as an off-white solid. An analytical sample

(23) Sanyal, I.; Mahroof-Tahir, M.; Nasir, M. S.; Ghosh, P.; Cohen, B. I.; Gultneh, Y.; Cruse, R. W.; Farooq, A.; Karlin, K. D.; Liu, S.; Zubieta, J. *Inorg. Chem.* **1992**, *31*, 4322.

(24) Lee, S. C.; Holm, R. H. *Inorg. Chem.* **1993**, *32*, 4745 and references therein.

(25) Hemmerich, P.; Sigwart, C. *Experientia* **1963**, *19*, 488.

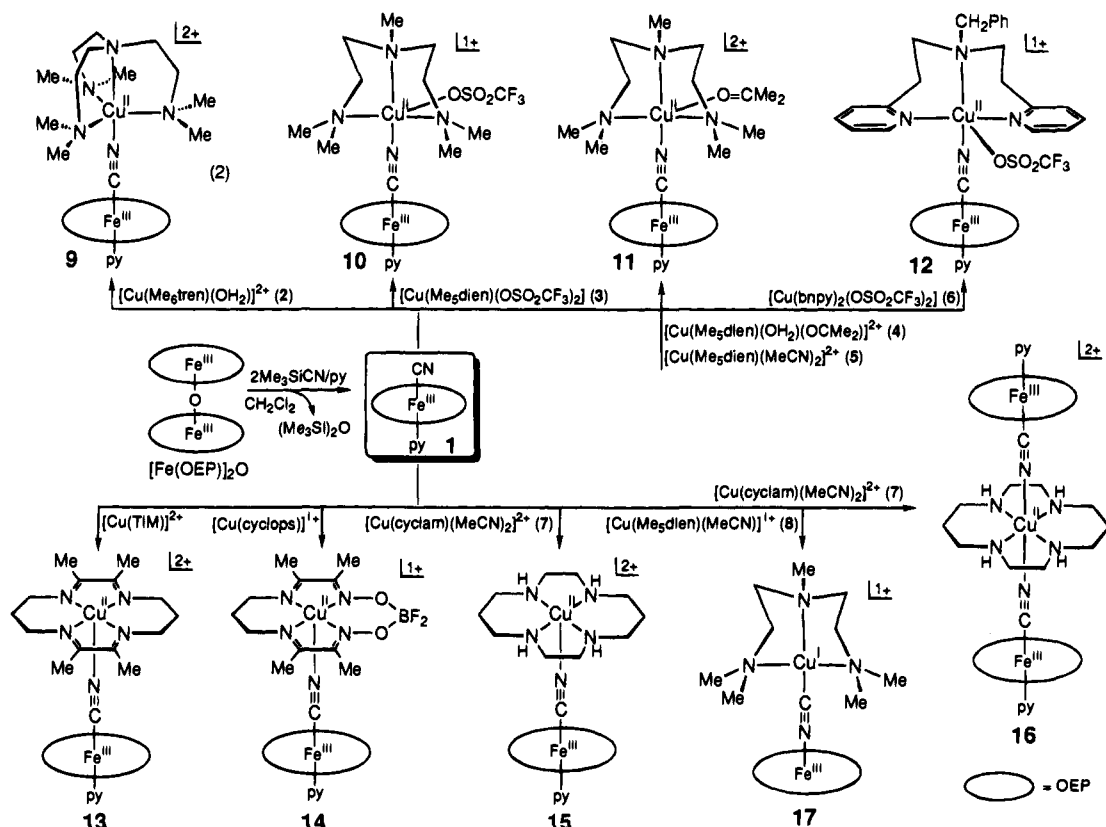


Figure 1. Synthesis of Fe-Cu cyanide-bridged assemblies **9**^{21,22} and **10-17** (this work) from heme complex **1** and the indicated Cu(II) precursors, including **2**,⁶ **3**,²² **5**,²² and **4** and **6-8** (this work). All reactions were carried out in acetone solution except those affording **15** and **16** (acetonitrile/dichloromethane) and **17** (acetonitrile). Accurate structures of all assemblies except **15** have been determined.

was recrystallized from acetonitrile/ether. Anal. Calcd for C₁₁H₂₆ClCuN₄O₄: C, 35.01; H, 6.94; Cu, 16.84; N, 14.85. Found: C, 35.09; H, 7.02; Cu, 16.89; N, 14.78.

(b) Bridged Assemblies. [(py)(OEP)Fe-CN-Cu(Me₅dien)(OSO₂CF₃)](CF₃SO₃). A solution of 94.8 mg (0.177 mmol) of [Cu(Me₅dien)(OSO₂CF₃)₂]²² in 2 mL of acetone was added to a solution of 123 mg (0.177 mmol) of [Fe(OEP)(CN)(py)]^{21,22} in 1 mL of acetone. The mixture was filtered, and several volume equivalents of ether were diffused into the filtrate. The product crystallized as large violet plates, but was contaminated with long blue needle-like crystals of {[Cu(Me₅dien)(OSO₂CF₃)₂(CN)](CF₃SO₃)}, which was identified by an X-ray structure determination.²⁶ The crystals were separated manually to afford 35 mg (16%) of product; atom ratios Fe:Cu:S = 1:1.1:1.9 by microprobe analysis. The compound has been identified by an X-ray structure determination.²²

[(py)(OEP)Fe-CN-Cu(Me₅dien)(OCMe₂)](ClO₄)₂. A solution of 30.9 mg (0.068 mmol) of [Cu(Me₅dien)(OH₂)](ClO₄)₂ in 0.5 mL of acetone was added to a solution of 47.2 mg (0.068 mmol) of [Fe(OEP)(CN)(py)] in 1 mL of acetone. The mixture was filtered, and several volume equivalents of ether were diffused into the filtrate. The dark violet crystalline mass was separated, washed with THF and ether, and dried in vacuo to afford 46 mg (57%) of product. Absorption spectrum²⁷ (acetone): λ_{max} (ε_M) 349 (32 000), 403 (101 000), 450 (sh, 9500), 526 (9600), 558 (sh, 6900) nm. Anal. Calcd for C₅₄H₇₈Cl₂CuFeN₉O₉: C, 54.62; H, 6.62; Cl, 5.97; Cu, 5.35; Fe, 4.70; N, 10.62. Found: C, 54.44; H, 6.65; Cl, 6.08; Cu, 5.29; Fe, 4.79; N, 10.49.

[(py)(OEP)Fe-CN-Cu(Me₅dien)(OCMe₂)](BF₄)₂·2Me₂CO. A mixture of 51.4 mg (0.074 mmol) of [Fe(OEP)(CN)(py)] and 36.5 mg (0.074 mmol) of [Cu(Me₅dien)(MeCN)₂](BF₄)₂²² was dissolved in 1

mL of acetone. The solution was filtered, and several volume equivalents of ether were diffused into the solution over 48 h. The solid was collected, washed with ether, and dried in vacuo to give 48 mg (53%) of product as large violet needle-like crystals. Absorption spectrum²⁷ (dichloromethane): λ_{max} (ε_M) 347 (36 000), 403 (95 700), 450 (sh, 9200), 524 (9400), 558 (sh, 6800). Anal. Calcd for C₅₇H₈₄B₂F₈CuFeN₉O₂: C, 56.10; H, 6.93; Cu, 5.21; Fe, 4.58; N, 10.33. Found: C, 56.62; H, 6.46; Cu, 5.14; Fe, 4.71; N, 10.24.

[(py)(OEP)Fe-CN-Cu(bnpy)₂(OSO₂CF₃)](CF₃SO₃). A mixture of 22.7 mg (0.033 mmol) of [Fe(OEP)(CN)(py)] and 22.0 mg (0.033 mmol) of [Cu(bnpy)₂(OSO₂CF₃)₂] was dissolved in a minimal volume (ca. 0.5 mL) of acetone. The solution was filtered, and several volume equivalents of ether were diffused into the filtrate. Large rhombohedral crystals of the product deposited from the reaction mixture and were isolated manually; atom ratios Fe:Cu:S = 1:1.1:2.0 by microprobe analysis. This compound was further identified by an X-ray structure determination.

[(py)(OEP)Fe-CN-Cu(TIM)](PF₆)₂. A mixture of 185 mg (0.267 mmol) of [Fe(OEP)(CN)(py)] and 160 mg (0.266 mmol) of [Cu(TIM)](PF₆)₂²⁸ was dissolved in a minimal amount (ca. 3 mL) of acetone. The dark violet solution was filtered, and the solvent was removed in vacuo. The solid residue was dissolved in dichloromethane, the solution was filtered, and the filtrate was taken to dryness in vacuo. The residue was dissolved in a minimal volume of acetone, and several volume equivalents of ether were diffused into the solution over 48 h. Very large, dark violet crystals of the product co-crystallized with blue needle-like crystals of [Cu(TIM)(py)](PF₆)₂.²⁸ The solid was collected, washed with ether, and manually separated to yield 181 mg (52%) of product. Absorption spectrum²⁷ (dichloromethane): λ_{max} (ε_M) 350 (25 700), 406 (86 500), 450 (sh, 10 000), 531 (8200), 563 (sh, 5400) nm. Anal. Calcd for C₅₆H₇₃CuF₁₂FeN₁₀P₂: C, 51.92; H, 5.68; Cu, 4.90; Fe, 4.31; N, 10.81; P, 4.78. Found: C, 51.84; H, 5.75; Cu, 4.98; Fe, 4.25; N, 10.78; P, 4.87.

[(py)(OEP)Fe-CN-Cu(cyclops)](ClO₄). A mixture of 61.0 mg (0.088 mmol) of [Fe(OEP)(CN)(py)] and 41 mg (0.088 mmol) of [Cu-

(26) This compound crystallizes in orthorhombic space group *Ama*2 with *a* = 20.84(1) Å, *b* = 24.43(2) Å, and *c* = 8.660(5) Å. The structure was solved, and the Cu^{II}-CN-Cu^{II} bridge was demonstrated. Full refinement was not performed inasmuch as we have reported a closely related compound with the same bridge.²²

(27) Absorption spectra are reported for use in compound identification; no investigation was made of potential dissociation at the submillimolar concentrations employed.

(28) Maroney, M. J.; Rose, N. J. *Inorg. Chem.* **1984**, *23*, 2252.

Table 1. Crystallographic Data^a for Cu(II,I) Complexes 4 and 6–8

	[4](ClO ₄)·H ₂ O	6	[7](CF ₃ SO ₃) ₂	[8](ClO ₄)
formula	C ₁₂ H ₃₃ Cl ₂ CuO ₁₁	C ₂₃ H ₂₃ CuF ₆ N ₃ O ₆ S ₂	C ₁₆ H ₃₀ CuF ₆ N ₆ O ₆ S ₂	C ₁₁ H ₂₆ ClCuN ₄ O ₄
formula wt	529.9	679.1	644.1	377.3
cryst syst	monoclinic	monoclinic	monoclinic	monoclinic
space group	<i>P</i> 2 ₁ / <i>n</i>	<i>P</i> 2 ₁ / <i>n</i>	<i>P</i> 2 ₁ / <i>n</i>	<i>P</i> <i>c</i>
<i>Z</i>	4	4	2	2
<i>a</i> , Å	8.616(3)	9.352(2)	8.009(3)	8.939(8)
<i>b</i> , Å	15.217(4)	20.557(6)	16.319(5)	7.577(7)
<i>c</i> , Å	18.011(6)	14.371(7)	10.384(3)	13.191(10)
β , deg	93.01(3)	96.66(2)	93.88(3)	102.77(7)
<i>V</i> , Å ³	2358(1)	2744(2)	1354(1)	871(1)
<i>T</i> , K	223	298	223	223
<i>d</i> _{calc} , g/cm ³	1.492	1.644	1.580	1.438
μ , mm ⁻¹	1.206	1.033	1.044	1.425
<i>R</i> ^b (<i>R</i> _w), ^c %	5.59 (6.14)	3.40 (3.78)	4.50 (4.99)	5.51 (5.92)

^a Obtained with graphite-monochromatized Mo K α radiation ($\lambda = 0.71073$ Å). ^b $R = \sum ||F_o| - |F_c|| / \sum |F_o|$. ^c $R_w = \{ \sum [w(|F_o| - |F_c|)^2 / \sum w|F_o|^2] \}^{1/2}$.

Table 2. Crystallographic Data^a for Fe–Cu Cyanide-Bridged Assemblies

	[11](SbF ₆) ₂ Me ₂ CO	[12](CF ₃ SO ₃)	[13](PF ₆) ₂ ·2Me ₂ CO	[14](SbF ₆)	[16](SbF ₆) ₂	[17](ClO ₄)
formula	C ₅₇ H ₈₄ CuF ₁₂ FeN ₉ O ₂ Sb ₂	C ₆₃ H ₇₂ CuF ₆ FeN ₉ O ₆ S ₂	C ₆₂ H ₈₅ CuF ₁₂ FeN ₁₀ O ₂ P ₂	C ₅₃ H ₆₇ BCuF ₈ FeN ₁₀ O ₂ Sb	C ₉₄ H ₁₂₂ CuF ₁₂ Fe ₂ N ₈ Sb ₂	C ₄₆ H ₆₇ ClCuFeN ₈ O ₄
formula wt	1518.2	1372.8	1411.7	1280.1	2121.8	950.9
cryst syst	triclinic	triclinic	monoclinic	monoclinic	monoclinic	triclinic
space group	<i>P</i> 1	<i>P</i> 1	<i>P</i> 2 ₁ / <i>c</i>	<i>P</i> 2 ₁ / <i>c</i>	<i>P</i> 2 ₁ / <i>n</i>	<i>P</i> 1
<i>Z</i>	2	2	4	4	2	2
<i>a</i> , Å	12.152(2)	14.960(6)	17.083(3)	13.619(3)	16.862(5)	12.265(3)
<i>b</i> , Å	13.658(3)	15.374(7)	18.220(4)	16.866(4)	17.419(3)	14.361(3)
<i>c</i> , Å	22.108(4)	16.233(5)	23.300(5)	26.053(4)	18.644(4)	15.066(4)
α , deg	82.04(3)	82.22(3)				98.69(2)
β , deg	89.41(3)	69.23(3)	109.40(3)	94.69(2)	112.68(2)	107.20(2)
γ , deg	67.11(3)	84.63(4)				104.93(2)
<i>V</i> , Å ³	3343(1)	3455(2)	6840(2)	5964(2)	5053(2)	2374(1)
<i>d</i> _{calc} , g/cm ³	1.508	1.320	1.371	1.426	1.395	1.330
μ , mm ⁻¹	1.405	0.649	0.651	1.115	1.088	0.860
<i>R</i> (<i>R</i> _w), ^b %	4.18 (4.27)	7.97 (8.52)	5.19 (5.71)	5.81 (5.62)	7.39 (8.16)	3.54 (3.80)

^a Obtained with graphite-monochromatized Mo K α radiation ($\lambda = 0.71073$ Å) at 223 K. ^b For definitions cf. Table 1.

(cyclops)](ClO₄)·H₂O²⁹ was dissolved in a minimal quantity of acetone. The dark red solution was stirred for several minutes and filtered, and several volume equivalents of ether were diffused into the filtrate. The solid was collected, washed with ether, and dried in vacuo to give 47 mg (49%) of product as large, dark violet, needle-like crystals that rapidly desolvated; atom ratios Fe:Cu:Cl = 1:1.0:1.1 by microprobe analysis. The compound was metathesized to the SbF₆¹⁻ salt for an X-ray structure determination; atom ratios Fe:Cu:Sb = 1:1.0:1.0.

{[(py)(OEP)Fe(CN)]₂Cu(cyclam)}(SbF₆)₂. A solution of 56.4 mg (0.100 mmol) of [Cu(cyclam)](CF₃SO₃)₂ in 0.5 mL of acetonitrile was added to a solution of 69.4 mg (0.100 mmol) of [Fe(OEP)(CN)(py)] and an excess of NaSbF₆ in 0.5 mL of dichloromethane. The solution was filtered, and several volume equivalents of ether were diffused into the filtrate. Over several days, large red crystals of the starting Cu(II) compound and small black crystals of the product precipitated. The latter were separated and analyzed; atom ratios Fe:Cu:Sb = 2:1.0:2.1 by microprobe analysis. The compound was further identified by an X-ray structure determination.

{(py)(OEP)Fe–CN–Cu(cyclam)}(ClO₄)₂. This compound has been isolated by use of a procedure similar to the preceding one, but with use of [Cu(cyclam)(MeCN)]₂(ClO₄)₂ and omission of NaSbF₆. The Cu(II) starting material was prepared analogously to [Cu(cyclam)](CF₃SO₃)₂ using [Cu(OH)₂]₆(ClO₄)₂; atom ratios Fe:Cu:S = 1:1.1:1.9 by microprobe analysis. The compound crystallized in a trigonal/hexagonal lattice with *a* = 21.629(5) Å and *c* = 21.497(6) Å (*T* = 223 K). The structure was solved in space group *P*3*c* and the cation was established to have a bridged structure. Refinement of the structure indicated that the crystal may have been twinned; no attempts were made to resolve the twin lattice, and, other than its infrared spectrum, and compound was not further characterized.

{(OEP)Fe–NC–Cu(Me₃dien)}(ClO₄)₂. A solution of 36.4 mg (0.096 mmol) of [Cu(Me₃dien)(MeCN)](ClO₄) in 0.3 mL of acetonitrile was added to a solution of 70.2 mg (0.101 mmol) of [Fe(OEP)(CN)(py)] in 0.3 mL of dichloromethane. The reaction mixture was stirred

for 30 s and filtered, and several volume equivalents of ether were diffused into the filtrate. A few large black crystals of the product and an amorphous precipitate were deposited from the solution over the course of several days. The solution was decanted, and the residue was washed with acetonitrile and ether. Large single crystals of product (10 mg) were collected. Attempts to improve the yield in this reaction system were not successful. Absorption spectrum²⁷ (dichloromethane): λ_{\max} (ϵ_M) 378 (84 000), 500 (8000), 540 (sh, 6500), 593 (sh, 3100), 643 (2700) nm. The compound was identified by an X-ray structure determination.

The preceding and other complexes of principal interest in this investigation are designated as follows:

[Fe(OEP)(py)(CN)]	1
[Cu(Me ₆ tren)(OH ₂)] ²⁺	2
[Cu(Me ₅ dien)(OSO ₂ CF ₃) ₂]	3
[Cu(Me ₅ dien)(OH ₂)(OCMe ₂)] ²⁺	4
[Cu(Me ₅ dien)(MeCN)] ₂ ²⁺	5
[Cu(bnpy ₂)(OSO ₂ CF ₃) ₂]	6
[Cu(cyclam)(MeCN)] ₂ ²⁺	7
[Cu(Me ₅ dien)(MeCN)] ⁺	8
{(py)(OEP)Fe–CN–Cu(Me ₆ tren)} ²⁺	9
{(py)(OEP)Fe–CN–Cu(Me ₃ dien)(OSO ₂ CF ₃) ⁺	10
{(py)(OEP)Fe–CN–Cu(Me ₃ dien)(OCMe ₂)] ²⁺	11
{(py)(OEP)Fe–CN–Cu(bnpy ₂)(OSO ₂ CF ₃) ⁺	12
{(py)(OEP)Fe–CN–Cu(TIM)} ²⁺	13
{(py)(OEP)Fe–CN–Cu(cyclops)} ⁺	14
{(py)(OEP)Fe–CN–Cu(cyclam)} ²⁺	15
{[(py)(OEP)Fe(CN)] ₂ Cu(cyclam)} ²⁺	16
{(OEP)Fe–NC–Cu(Me ₃ dien)} ⁺	17
{[(OEP)Fe(CN)] ₂ [Cu(Me ₆ tren)] ₂ } ³⁺	18

X-ray Data Collection and Reduction. Structures of the four copper complexes in Table 1 and the six bridged assemblies in Table 2 have been determined. For brevity in this section, all compounds in these tables which are salts are referred to by their cation number. Suitable crystals were grown by vapor diffusion of ether in a saturated

(29) Addison, A. W.; Carpenter, M.; Lau, L. K.-M.; Wicholas, M. *Inorg. Chem.* 1978, 17, 1545.

solution of the compound in acetone (**4**, **6**, **7**, **11–14**), acetonitrile (**8**, **17**), or acetonitrile/dichloromethane (1:1 v/v) (**16**). A small amount of NaSbF₆ was added to solutions containing **11**, **14**, and **16**. Single crystals were coated with Paratone-N oil and attached to glass fibers. The crystals were transferred to a Nicolet R3mv diffractometer and cooled with a nitrogen stream.

Lattice parameters were obtained from a least-squares analysis of carefully centered reflections with $15^\circ \leq 2\theta \leq 30^\circ$. Decay corrections were based on the measured intensities of two reflections monitored periodically throughout the course of data collection; no significant decay was observed for any sample. The raw intensity data were converted to structure factor amplitudes and their esd's by correction for scan speed, background, and Lorentz and polarization effects using the program XDISK of the SHELXTL PLUS program package. An empirical absorption correction based on the observed variation in intensity of azimuthal scans (ψ scans) was applied to the data sets using the program XEMP. Compounds **4**, **6–8**, **13**, **14**, and **16** crystallize in a monoclinic system; systematic absences identified the space group as $P2_1/n$ (**4**, **6**, **7**, **16**), Pc (**8**), and $P2_1/c$ (**13**, **14**). Compounds **11**, **12**, and **17** crystallize in a triclinic system; the space group $P1$ was assigned to each on the basis of statistics and successful refinements of the structures.

Structure Solution and Refinement. Structures were solved by direct methods or from a Patterson map using standard procedures and were refined via full matrix least-squares and Fourier techniques using the SHELXTL PLUS package. All non-hydrogen atoms were refined with anisotropic thermal parameters unless otherwise noted. Hydrogen atoms were assigned idealized locations and given a uniform value for B_{iso} .

The asymmetric unit of **4** consists of one cation and two anions and water molecule, while the asymmetric unit of **6** consists of one complete molecule. The cation of **7** crystallizes on an inversion center, and the anion resides on a general position. The asymmetric unit of **8** contains one cation and one anion. Compound **11** crystallized with one cation, one complete anion, two half-anions, and a solvate molecule in the asymmetric unit. The anions crystallize on a general position and on the two inversion centers. In compound **12**, the coordinated triflate anion is disordered over two positions each with a site occupancy factor of 0.5. The Cu-bound oxygen atom and the sulfur atom were refined anisotropically with a site occupancy factor of 1.0; in addition, the S–C distance was constrained to be 1.86 Å. Disorder also occurs in the ethyl groups of the porphyrin. Two groups were constrained to have C–C distances of 1.54 Å, and one methyl group was refined with two positions, each with an occupancy factor of 0.5. Because of the limited data ($F_o^2 > 3\sigma(F_o^2)$), all carbon atoms, except for that of the cyanide group, were refined isotropically. The asymmetric unit of **13** contains one cation, two anions, and two acetone solvate molecules; the latter were refined isotropically. For **14**, the asymmetric unit contains one anion and one cation. One of the ethyl groups of the porphyrin is disordered over two positions; the methyl group was refined isotropically with occupancy factors of 0.5. The copper atom of **16** crystallizes on an inversion center and the anion on a general position. Compound **17** crystallizes with one anion and one cation in the asymmetric unit. Both orientations of the cyanide bridges were analyzed in the final stages of refinement of **11–14**, **16**, and **17**. In every case except **17** the sequence Fe–C–N–Cu was favored over Fe–N–C–Cu. In the last cycle of refinement of all structures, all parameters shifted by <1% of the esd of the parameter, and final difference parameters showed no significant electron density. Final agreement factors are contained in Tables 1 and 2.³⁰

Other Physical Measurements. Absorption spectra were recorded on a Perkin-Elmer Lambda 4C spectrophotometer. IR spectra were determined with a Nicolet IR/42 spectrometer. Microprobe analyses were performed on crystalline samples by a Cameca MBX electron microprobe using a Tracor Northern TH-1310 wavelength-dispersive spectrometer with a TN-5502 EDS system and a stage automation system.

Results and Discussion

Preparation of Compounds. The synthesis of bridged assemblies **9–17** is summarized in Figure 1, which also conveys

(30) See paragraph at the end of this article concerning supplementary material.

Table 3. Selected Interatomic Distances (Å) and Angles (deg) of Cu(II,I) Complexes **4** and **6–8**

[Cu(Me ₅ dien)(OH ₂)(OCMe ₂) ²⁺ (4)			
Cu–O(2)	2.222(6)	N(2)–Cu–N(3)	86.2(2)
Cu–O(1)	1.994(6)	O(2)–Cu–O(1)	89.0(2)
Cu–N(1)	2.036(7)	O(2)–Cu–N(1)	104.1(2)
Cu–N(2)	2.022(6)	O(2)–Cu–N(2)	98.9(2)
Cu–N(3)	2.034(6)	O(2)–Cu–N(3)	96.7(2)
O(1)–Cu–N(3)	92.8(2)	N(1)–Cu–N(3)	158.8(3)
O(1)–Cu–N(1)	91.8(2)	O(1)–Cu–N(2)	172.1(2)
N(1)–Cu–N(2)	86.4(3)		
[Cu(bnpy ₂)(OSO ₂ CF ₃) ₂] ²⁺ (6)			
Cu–O(21)	2.251(4)	N(2)–Cu–N(3)	87.4(2)
Cu–O(11)	2.038(4)	O(21)–Cu–O(11)	91.1(1)
Cu–N(1)	2.016(4)	O(21)–Cu–N(1)	88.6(2)
Cu–N(2)	2.081(4)	O(21)–Cu–N(2)	102.9(1)
Cu–N(3)	1.989(4)	O(21)–Cu–N(3)	96.3(2)
O(11)–Cu–N(3)	88.2(2)	O(11)–Cu–N(2)	165.7(1)
O(11)–Cu–N(1)	87.5(1)	N(1)–Cu–N(3)	173.5(2)
N(1)–Cu–N(2)	95.7(2)		
[Cu(cyclam)(MeCN) ₂] ²⁺ (7)			
Cu–N(1)	2.020(4)	N(3)–Cu–N(1)	87.3(2)
Cu–N(2)	2.023(4)	N(3)–Cu–N(2)	91.6(2)
Cu–N(3)	2.570(5)	N(3)–Cu–N(1')	92.7(2)
N(1)–Cu–N(2)	86.0(2)	N(3)–Cu–N(2')	88.4(2)
N(2)–Cu–N(1')	94.0(2)		
[Cu(Me ₅ dien)(MeCN)] ¹⁺ (8)			
Cu–N(1)	2.04(1)	N(1)–Cu–N(2)	87.2(4)
Cu–N(2)	2.19(1)	N(2)–Cu–N(3)	84.6(4)
Cu–N(3)	2.18(1)	N(1)–Cu–N(3)	120.6(4)
Cu–N(4)	1.93(1)	N(1)–Cu–N(4)	128.4(5)
		N(2)–Cu–N(4)	118.5(4)
		N(3)–Cu–N(4)	106.6(5)

the compound numbering scheme. The preparation and structure of **9** and **18** and the structure of **10** have been described earlier.^{21,22} All assemblies were prepared by the reaction of heme complex **1** with an appropriate Cu(II,I) precursor **2–8**, [Cu(TIM)]²⁺, or [Cu(cyclops)]⁺ selected so as to vary the copper site stereochemistry. The reactions proceed by substitution of a labile ligand (water, acetone, triflate, acetonitrile) from a copper site by the N-end of the cyanide group of **1** in a solvent of low coordinating tendency (acetone). Because structural definition is the principal goal in this phase of the research on cyanide-bridged complexes, preparations were conducted on a scale and in a manner intended to obtain diffraction-quality crystals directly from reaction mixtures. In some cases, starting materials and/or unidentified byproducts co-crystallized with the desired product, which, however, could be recovered in reasonable yield by manual separation based on color and crystal habit. Compounds were identified by a combination of elemental analysis, atom ratios determined by microprobe analysis, and X-ray structure determinations. Complexes **11**, **14**, and **16** were metathesized to [SbF₆][−] salts to obtain crystals suitable for X-ray work. In the case of [17](ClO₄), which thus far has been isolated in very low yield, the compound was characterized by a structure determination only.

Prior to a consideration of the bridged assemblies themselves, we examine briefly the structures of precursor Cu(II,I) complexes. The structures of trigonal bipyramidal (TBP) **2** and distorted square pyramidal (d-SP) **3** and **5**, in which the two monodentate ligands occupy an axial and an equatorial position, have been determined previously.²²

Structures of Cu(II,I) Complexes. The structures of **4**, **6**, **7**, and **8** are shown in Figure 2; selected metric parameters are collected in Table 3. In the case of complex **4**, the bond angles O(1)–Cu–N(2) = 172.1(2)° and N(1)–Cu–N(3) = 158.8(3)°, the long Cu–O(2) distance of 2.222(6) Å, and the range 89.0–(2)–104.1(2)° for the four bonded angles involving O(2) denote

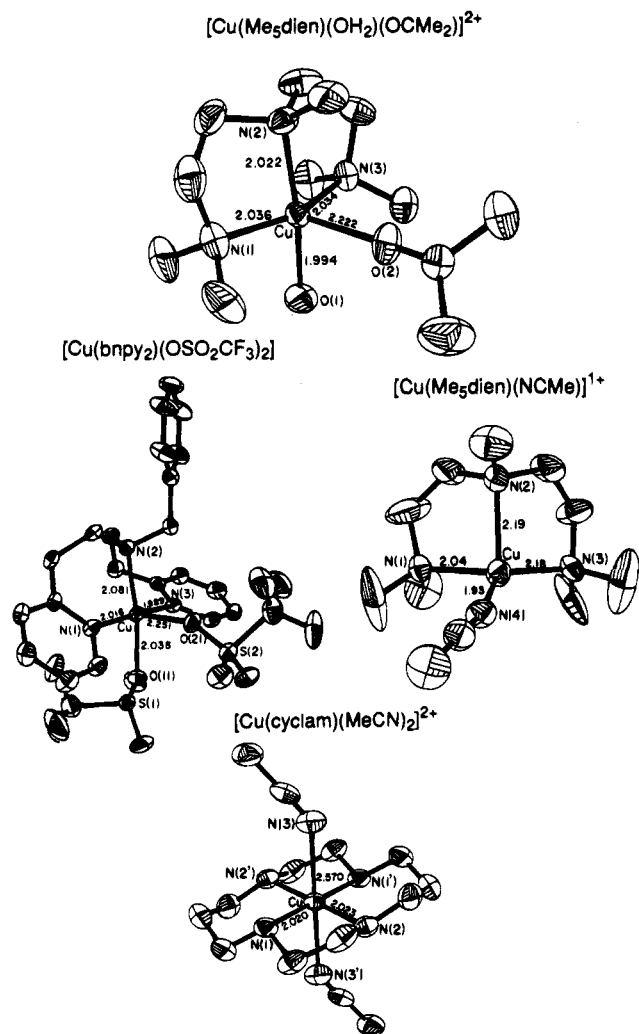


Figure 2. Structures of Cu(II,I) precursor complexes **4** and **6–8** showing 50% probability ellipsoids and selected bond distances; primed and unprimed atoms in **7** are related by an inversion center.

the stereochemistry as d-SP. The acetone ligand is in the axial position, and the water molecule is in an equatorial position. The structure is very similar to that of **3** and of **5**; as a set these complexes reveal the strong preference of the Me₅dien ligand for equatorial binding in five-coordinate Cu(II) complexes, leaving an axial or equatorial site susceptible to ligand substitution. By a similar argument, complex **6** has a d-SP structure with a triflate ligand in the axial position at the bond length Cu–O(21) = 2.251(4) Å. This is the same type of stereochemistry found with other Cu(II)–bnpy₂ complexes.²⁴ Complex **7** has a tetragonal centrosymmetric configuration with two acetonitrile molecules weakly coordinated at Cu–N(3) = 2.570(5) Å, a distance at the end of the range (2.35–2.57 Å) of axial interactions previously observed in Cu(II)–cyclam complexes.³¹ Of the remaining Cu(II) starting materials, [Cu(TIM)]²⁺ is planar and binds axial ligands to form SP complexes;^{27,32} the latter includes the N-bound complex [Cu(TIM)(NCS)]⁺.^{32b} The structure of [Cu(cyclops)]⁺ has not been determined; by analogy with [Cu(TIM)]²⁺ and the SP structures of [Cu(cyclops)L]^{+,0,33} including N-bound [Cu(cyclops)(NCO)],^{33a} it is expected to be

(31) (a) Tasker, P. A.; Sklar, L. *J. Cryst. Mol. Struct.* **1975**, *5*, 329. (b) Kato, M.; Ito, T. *Bull. Chem. Soc. Jpn.* **1986**, *59*, 285. (c) Emsley, J.; Arif, M.; Bates, P. A.; Hursthouse, M. B. *J. Mol. Struct.* **1990**, *220*, 1.

(32) (a) Elia, A.; Santasiero, B. D.; Lingafelter, E. C.; Schomaker, V. *Acta Crystallogr.* **1982**, *B38*, 3020. (b) Elia, A.; Lingafelter, E. C.; Schomaker, V. *Acta Crystallogr.* **1984**, *C40*, 1313.

(33) (a) Anderson, O. P.; Marshall, J. C. *Inorg. Chem.* **1978**, *17*, 1258; (b) **1979**, *18*, 1940; **1980**, *19*, 2123. (c) Anderson, O. P.; Packard, A. B. *Inorg. Chem.* **1980**, *19*, 2941.

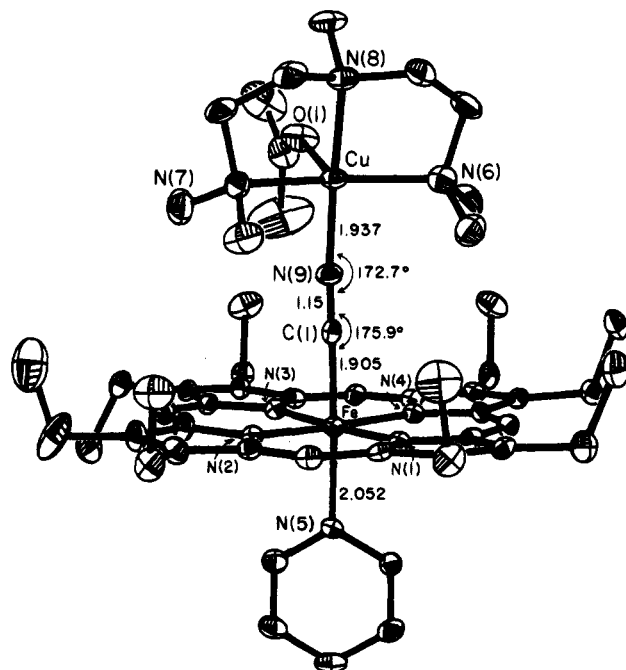
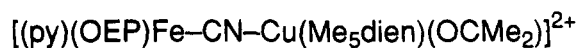


Figure 3. Structure of bridged assembly **11**, showing 30% probability ellipsoids and bond distances and angles in the [Fe^{III}–CN–Cu^{II}] bridge region.

planar. Thus, [Cu(cyclam)]²⁺, [Cu(TIM)]²⁺, and [Cu(cyclops)]⁺ have well-documented affinities for axial N-donor ligands, albeit at different bond lengths and with variable displacements of the Cu(II) atom from the macrocyclic N₄ plane.

Copper(I) complex **8** has a structure so irregular that it cannot be described as distorted tetrahedral. Chelate ring bond angles N(1)–Cu–N(2) = 87.2(4)° and N(2)–Cu–N(3) = 84.6(4)° are comparable to those in **3–5** and are largely set by ligand structure. The four other bond angles at Cu are much larger and occur in the range 106.6(5)–128.4(5)°. Together with the short Cu–N(1) bond distance of 2.04(1) Å, these parameters void even an idealized C₃ structure description. As will be seen, peculiar distortions persist in the Cu(Me₅dien)⁺ fragment incorporated into its bridged assembly.

Fe^{III}–CN–Cu^{II} Bridged Assemblies. The structures of monobridged **11–14** and dibridged **16** have been determined. Structures are set out in Figures 3–7, and selected interatomic distances and angles are collected in Tables 4 and 5.

(a) **Heme Fragments.** The structure of complex **1** has been determined at 293 K³⁴ and is prototypical of low-spin ferrihemes. Significant metric features are mean Fe–N_p = 1.980(4) Å, Fe–CN = 1.934(4) Å, Fe–N(py) = 2.087(3) Å, Fe–C–N = 179.1(1)°, and Fe–Ct = 0.053 Å. The Fe–N_p distance and the small out-of-plane displacement of the Fe atom are structurally diagnostic for low-spin Fe(III).³⁵ The following ranges of values have been observed for **11–14** and **16**: mean Fe–N_p = 1.95(1)–1.99(1) Å, Fe–CN = 1.86(3)–1.92(1) Å, Fe–N(py) = 2.05(1)–2.11(1) Å, and Fe–C–N = 176(1)–179(1)°. Out-of-plane displacements are small and, with one exception (**13**), are in the direction of the pyridine nitrogen atom. The results are consistent only with low-spin Fe(III) and demonstrate, with the exception of a change in direction of the Fe atom displacement, that the Fe(OEP)(py)(CN) fragment in the bridged assemblies is essentially congruent with **1**. The same conclusion has been reached for the fragments present in **9** and **10**.²²

(34) Scheidt, W. R.; Hatano, K. *Acta Crystallogr.* **1991**, *C47*, 2201.

(35) Scheidt, W. R.; Reed, C. A. *Chem. Rev.* **1981**, *81*, 543.

Table 4. Selected Interatomic Distances (Å) and Angles (deg) of Fe^{III}-CN-Cu^{II} Bridged Assemblies 11-13

	11	12	13
bridge			
Fe-C(1)	1.905(8)	1.86(3)	1.912(7)
C(1)-N(9/10) ^a	1.15(1)	1.13(3)	1.150(9)
Cu-N(9/10)	1.937(7)	2.02(2)	2.171(7)
Fe-C(1)-N(9/10)	175.9(7)	176(1)	179.0(6)
Cu-N(9/10)-C(1)	172.7(6)	163(1)	147.3(5)
Fe··Cu	4.98	4.94	5.02
Fe··Ct ^b	0.109	0.01	-0.003
heme			
Fe-N(1)	1.996(6)	1.95(1)	1.976(5)
Fe-N(2)	1.994(7)	1.94(2)	1.971(5)
Fe-N(3)	1.980(6)	1.93(1)	1.977(5)
Fe-N(4)	1.993(7)	1.96(1)	1.973(5)
mean of 4	1.991(7)	1.95(1)	1.974(3)
Fe-N(5)	2.052(6)	2.07(1)	2.072(5)
N _p -Fe-N _p ^c mean	90.0(2)	90.0(6)	90.0(2)
N _p -Fe-N(5) mean	90.9(4)	87(2)	90(2)
C(1)-Fe-N(5)	176.4(3)	174.2(6)	178.3(2)
Cu fragment			
Cu-N(6)	2.042(9)	1.99(1)	1.978(5)
Cu-N(7)	2.053(9)	1.99(1)	1.971(6)
Cu-N(8)	2.037(7)	2.09(1)	1.965(5)
Cu-O(1/11) ^d	2.294(6)	2.34(1)	
Cu-N(9)			1.967(6)
N(6)-Cu-N(8)	86.6(3)	94.9(5)	164.9(3)
N(7)-Cu-N(8)	87.0(3)	88.8(5)	80.8(2)
N(6)-Cu-N(9)	91.6(3)	89.9(5)	80.7(2)
N(7)-Cu-N(9)	92.2(3)	87.5(5)	168.7(3)
O(1/11)-Cu-N(9)	92.8(2)	100.0(6)	
O(1/11)-Cu-N(8)	93.4(2)	105.8(5)	
O(1/11)-Cu-N(7)	99.9(3)	89.2(5)	
O(1/11)-Cu-N(6)	105.2(3)	88.2(5)	
N(8)-Cu-N(9)	173.8(3)	153.9(7)	97.8(2)
N(6)-Cu-N(7)	154.4(3)	175.9(6)	97.7(2)
N(10)-Cu-N(6-9) range			92.5(2)-102.5(2)

^a N(10) in **13**. ^b Displacement (Å) from the porphyrin plane toward N(5). ^c N_p = porphyrin nitrogen atoms. ^d O(11) in **12**.

(b) Cu(II) Fragments. In assemblies **11** and **12**, the pattern of bond distances and angles clearly shows that the d-SP stereochemistry of precursors **3**²² and **6**, respectively, is retained. The Cu-O(1) distance of 2.294(6) Å in **11** (Figure 3) and the Cu-O(11) distance of 2.34(1) Å in **12** (Figure 4) define the axial directions in these complexes. Consequently, N-bonded cyanide occupies equatorial positions with bond distances Cu-N(9) = 1.937(7) Å in **11** and Cu-N(9) = 2.02(2) Å in **12**. With regard to stereochemistry at the Cu(II) center, these bridged assemblies are analogous to **10**, in which triflate occupies the axial position at a Cu-O bond length of 2.239(6) Å and N-bound cyanide an equatorial position at a Cu-N distance of 1.949(5) Å.

In assemblies **13** and **14**, N-bound cyanide occupies an axial position with a Cu-N bond essentially perpendicular to the N₄ mean plane. In the case of **13** (Figure 5), the mean Cu-N macrocyclic distance of 1.970(6) Å is unimportantly different from that of precursor **7** (2.022 Å). Bridge formation results in forging of the Cu-N(10) bond at 2.171(7) Å and the accompanying displacement of the Cu(II) atom from the N₄ mean plane toward the axial ligand by 0.226 Å. The SP stereochemistry around Cu(II) is similar to that in [Cu(TIM)(NCS)]⁺, but in this complex the axial Cu-N bond is much longer (2.38(1) Å) and the out-of-plane displacement smaller (0.07 Å).^{34b} The situation differs to the extent that the axial ligand is not bound linearly (Cu-N-C = 123(1)°) and the terminal sulfur atom interacts (weakly) with a Cu(II) atom in another molecule. In **14** (Figure 6), the Cu(II) coordination unit is also SP as in [Cu(cyclops)L]^{0,+} complexes.^{29,33} Bridge formation involves the Cu-N(10) bond at 2.13(1) Å and a substantial displacement of the Cu(II) atom from the N₄ plane

Table 5. Selected Interatomic Distances (Å) and Angles (deg) of Fe^{III}-CN-Cu^{II} Bridged Assemblies **14** and **16** and Fe^{III}-NC-Cu^I Bridged Assembly **17**

	14	16	17
bridge			
Fe-C(1)	1.92(1)	1.91(1)	
Fe-N(5)			1.998(3)
C(1)-N(5/8/10) ^a	1.15(2)	1.14(2)	1.138(4)
Cu-N(8/10)	2.13(1)	2.45(1)	
Cu-C(1)			1.859(3)
Fe-C(1)-N(8/10)	178.6(9)	177(1)	
Fe-N(5)-C(1)			165.3(4)
Cu-N(8/10)-C(1)	159.5(9)	139.8(9)	
Cu-C(1)-N(5)			168.9(4)
Fe··Cu	5.11	5.15	4.90
Fe··Ct ^b	0.031	0.088	0.34
heme			
Fe-N(1)	1.978(9)	2.003(8)	2.045(3)
Fe-N(2)	1.997(8)	1.974(8)	2.043(3)
Fe-N(3)	1.997(9)	1.990(8)	2.038(3)
Fe-N(4)	1.991(9)	1.998(9)	2.035(3)
mean of 4	1.991(9)	1.99(1)	2.040(5)
Fe-N(5)	2.11(1)	2.07(1)	
N _p -Fe-N _p ^c mean	90.0(4)	90.0(5)	88.3(2)
N _p -Fe-N(5) mean	90.2(7)	90.4(9)	99(1)
C(1)-Fe-N(5)	179.1(4)	178.5(4)	
Cu fragment			
Cu-N(6)	1.98(1)	2.01(1)	2.229(4)
Cu-N(7)	1.953(9)	2.02(1)	2.091(3)
Cu-N(8)	1.98(1)		2.152(4)
Cu-N(9)	1.95(1)		
N(6)-Cu-N(7)	80.7(4)	93.5(4)	85.2(1)
N(7)-Cu-N(8)	97.7(4)	91.7(4)	85.1(1)
N(8)-Cu-N(9/6') ^d	81.1(4)	86.6(5)	
N(6)-Cu-N(9)	92.6(4)		
N(8)-Cu-N(6)	159.2(4)	93.4(5)	113.0(2)
N(7)-Cu-N(9/6')	157.8(4)	86.5(4)	
N(8)-Cu-N(7')		88.3(4)	
N(6)-Cu-C(1)			110.1(2)
N(7)-Cu-C(1)			146.7(2)
N(8)-Cu-C(1)			113.4(2)
N(10)-Cu-N(6-9) range	92.0(4)-110.2(4)		

^a N(5) in **17**, N(8) in **16**. ^b Displacement (Å) from porphyrin mean plane toward N(5). ^c N_p = porphyrin nitrogen atoms. ^d Primed atoms are in **16**.

toward the axial ligand by 0.36 Å. The macrocyclic mean Cu-N distance of 1.97(2) Å is normal. The most closely related mononuclear complex is [Cu(cyclops)(NCO)],^{33a} whose equatorial mean Cu-N bond is essentially the same (2.001(8) Å), but whose axial Cu-N bond is somewhat shorter (2.038(4) Å) and out-of-plane displacement larger (0.58 Å). Large displacements appear to be an inherent property of SP Cu(II)-cyclops complexes.³³ Complex **15** was shown to have SP stereochemistry at the Cu(II) site, but poor crystal quality precluded an accurate refinement of the structure. In the doubly bridged complex **16** (Figure 7), the copper atom resides on a symmetry center and exhibits tetragonally distorted octahedral (TO) geometry. The macrocyclic distances and angles and the Cu-N(8) distance of 2.45(1) Å are consistent with known Cu(II)-cyclam complexes.³¹ This bond distance is 0.12 Å shorter than the axial bonds in **7**, presumably because of the anionic nature of the ligand.

(c) [Fe^{III}-CN-Cu^{II}] Bridges. In bridged assemblies **9-14** and **16**, the structure refinement indicated that the carbon atom of the cyanide moiety is bound to the Fe atom. The Fe-CN distances (1.86(3)-1.92(1) Å) and Fe-C-N angles (176(1)-179(1)°) show only minor variations over the series of compounds. However, the Cu-NC distances and Cu-N-C angles vary markedly. In **9**, where the ligand is in the TBP-axial position, the bridge is nearly linear (174(1)°). This is also the case for the d-SP-equatorial assemblies **10** (170.2(5)°) and **11** (172.7(6)°). In these three species the Cu-NC bond lengths

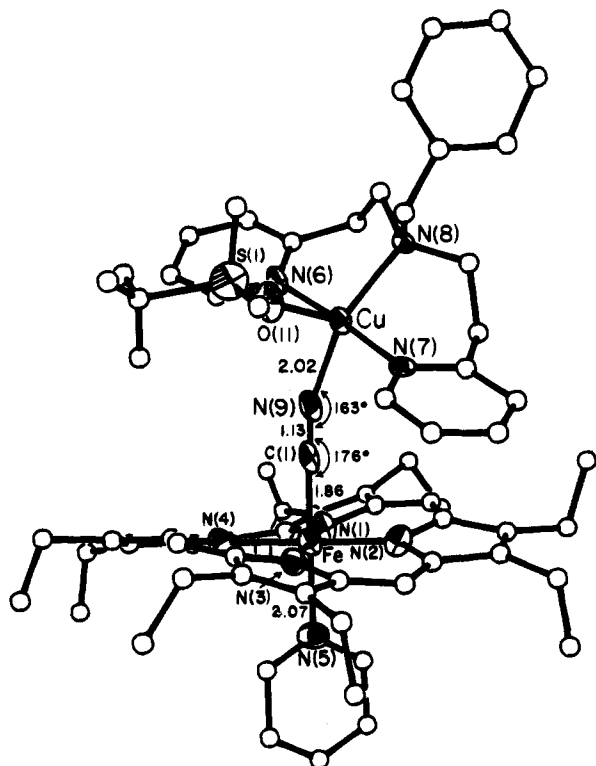
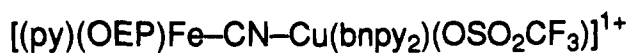


Figure 4. Structure of bridged assembly 12, showing 30% probability ellipsoids and bond distances and angles in the $[\text{Fe}^{\text{III}}-\text{CN}-\text{Cu}^{\text{II}}]$ bridge region. For clarity, only one of the two refined orientations of the triflate ligand is shown; open circles (arbitrary radii) indicate atoms that were refined isotropically.

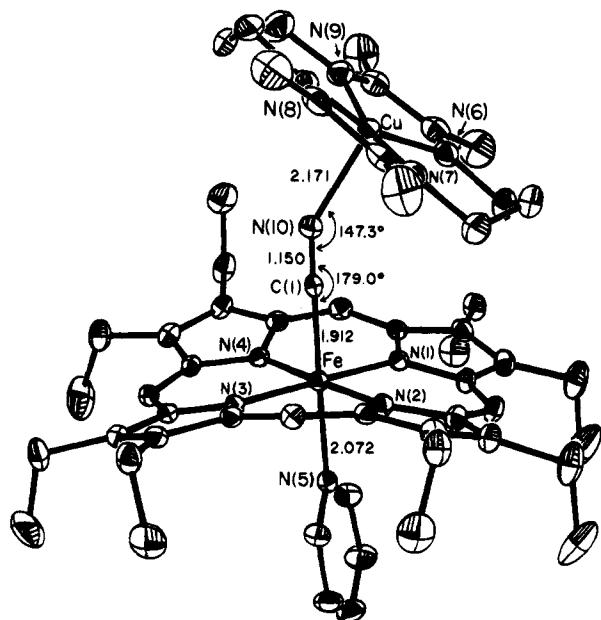
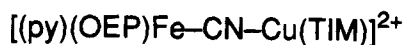


Figure 5. Structure of bridged assembly 13, showing 30% probability ellipsoids and bond distances and angles in the $[\text{Fe}^{\text{III}}-\text{CN}-\text{Cu}^{\text{II}}]$ bridge region.

occur in the interval 1.90(1)–1.949(5) Å. The situation is quite different in the d-SP-equatorial species 12, whose bridge is appreciably bent (163(1)°) with a longer bond (2.02(2) Å). SP-axial assemblies 14 (159.5(9)°, 2.13(1) Å) and 13 (147.3(5)°, 2.171(7) Å) further indicate a trend of decreasing Cu–N–C

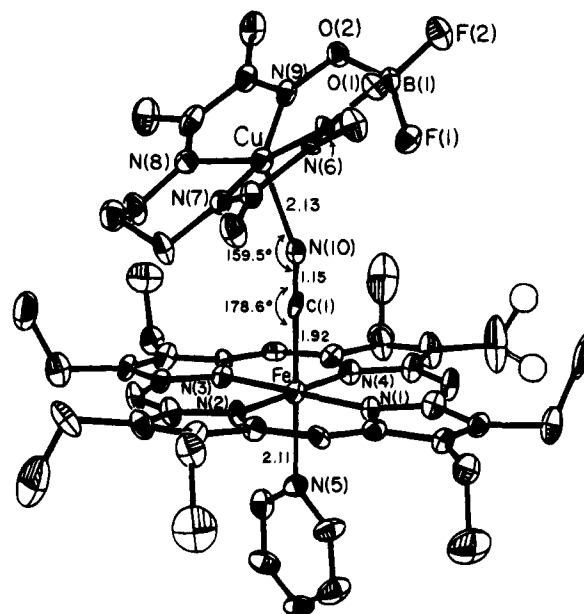


Figure 6. Structure of bridged assembly 14, showing 30% probability ellipsoids and bond distances and angles in the $[\text{Fe}^{\text{III}}-\text{CN}-\text{Cu}^{\text{II}}]$ bridge region. The open circles represent two orientations of an isotropically refined methyl group.

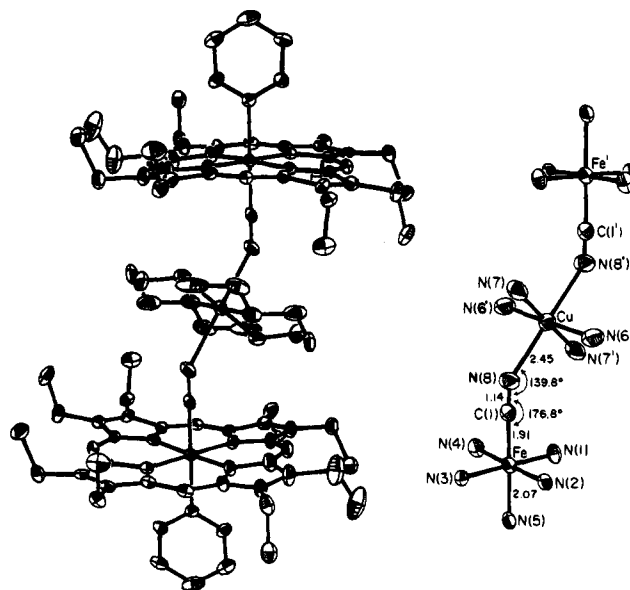


Figure 7. Structure of doubly bridged assembly 16, showing 30% probability ellipsoids and bond distances and angles in the $[\text{Fe}^{\text{III}}-\text{CN}-\text{Cu}^{\text{II}}]$ region; primed and unprimed atoms are related by an inversion center.

bridge angle with increasing Cu–NC bond length. The limit is reached with doubly bridged 16 with Cu–N–C = 139.8(9)° and Cu–NC = 2.45(1) Å. The related centrosymmetric doubly bridged assembly 18, which has the bridge sequence $\text{Cu}^{\text{II}}-\text{NC}-\text{Fe}^{\text{III}}-\text{CN}-\text{Cu}^{\text{II}}$, does not adopt a bent stereochemistry, but instead resembles 9 (171.8(9)°, 1.94(1) Å).²²

(d) $[\text{Fe}^{\text{III}}-\text{NC}-\text{Cu}^{\text{I}}]$ Bridge. The structure of 17 is shown in Figure 8; structure refinement clearly favored the indicated bridge atom sequence in which the cyanide has inverted its connectivity to the Fe and Cu sites. Selected interatomic distances and angles are collected in Table 5. The large out-of-plane displacement of the iron atom from the porphyrin plane toward N(5) (0.34 Å) and the long Fe–N_p distance (2.040(5)

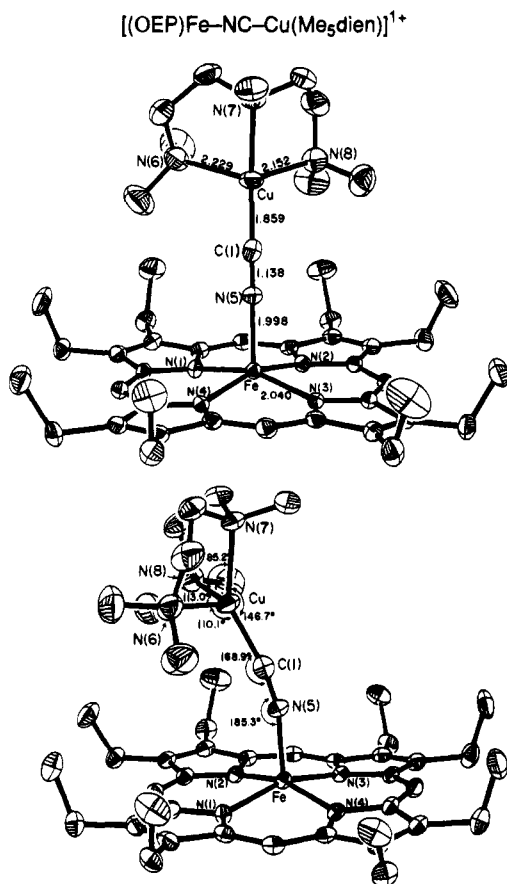


Figure 8. Two views of the structure of bridged assembly 17, showing 30% probability ellipsoids and bond distances and angles in the [Fe^{III}-NC-Cu^I] region and at the Cu(I) site.

Å) are indicative of a high-spin Fe(III) heme.³⁵ As is the case for 8, the copper(I) fragment in the bridged complex lacks any definable geometry. The chelate ring bond angles N(6)-Cu-N(7) = 85.2(1)° and N(7)-Cu-N(8) = 85.1(2)° are consistent with those in 3-5 and 8, whereas the four other bond angles vary over a wide range from 110.1(2)° to 146.7(2)°. There is also a large disparity in the Cu-N bond distances, which range from 2.091(3) to 2.229(4) Å and are slightly longer than the corresponding distances in 8. The Cu-C(1) bond (1.859(3) Å) is shorter than the corresponding Cu-N(4) distance (1.93(1) Å) in 8, and it is also the shortest metal-cyanide bond found in any of the complexes 9-16. This bond length compares closely with the values found in polymerized trigonal Cu(I) cyanides (1.86-1.90 Å)³⁶ and is close to the value of 1.91(2) Å for a tetrahedral Cu^I-CN-Cu^{II} bridge.³⁷ As expected, this distance is also significantly shorter than those found in Cu(II)-cyanide complexes containing Me₅dien and Me₆tren ligands.²² Unlike the Fe^{III}-CN-Cu^{II} bridged assemblies, the cyanide moiety in 17 contains two bent M-cyanide bonds with Fe-N(5)-C(1) = 165.3(4)° and Cu-C(1)-N(5) = 168.9(4)°. Note that the complex was prepared by the reaction of heme complex 1 and Cu(I) species 8 in a process requiring the inversion of cyanide, possibly after displacement of acetonitrile. This is the only example of the Fe-NC-Cu bridge we have encountered. As noted earlier,²¹ reaction of [Fe(OEP)(OCIO₃)] with [Cu(Me₆tren)(CN)]⁺, containing the Cu-CN bond,²² in

(36) (a) Cromer, D. T.; Larson, A. C. *Acta Crystallogr.* **1962**, *15*, 397; **1972**, B28, 1052. (b) Dyason, J. C.; Healy, P. C.; Engelhardt, L. M.; Pakawatchai, C.; Patrick, V. A.; White, A. H. *J. Chem. Soc., Dalton Trans.* **1985**, 839. (c) Dessy, G.; Fares, V.; Imperatori, P.; Morpurgo, G. O. *J. Chem. Soc., Dalton Trans.* **1985**, 1285.

(37) Agnus, Y.; Gisselbrecht, J. P.; Louis, R.; Metz, B. *J. Am. Chem. Soc.* **1989**, *111*, 1494.

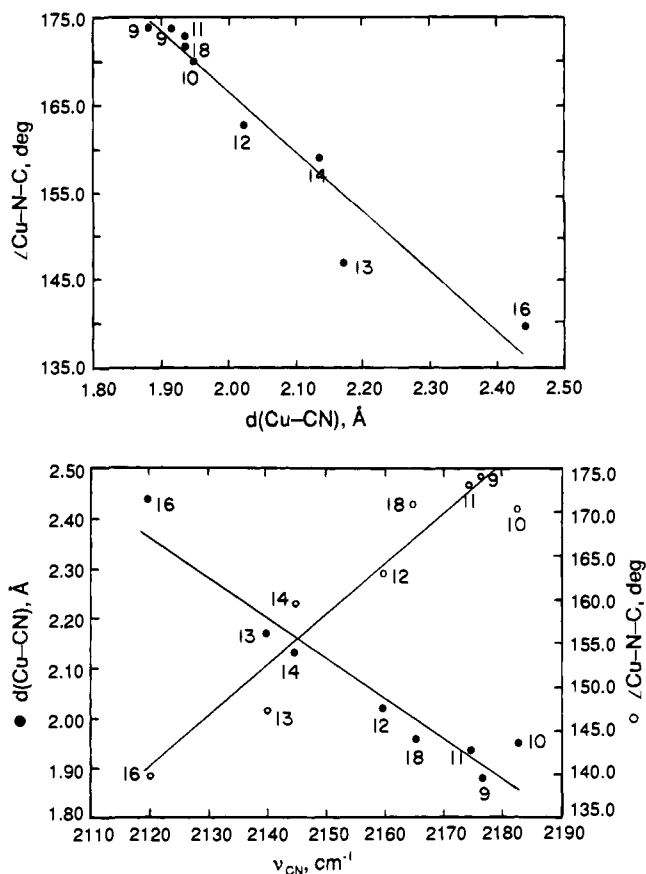


Figure 9. Correlation plots for [Fe^{III}-CN-Cu^{II}] monobridged (9-14) and dibridged assemblies (16, 18). Upper: trend of decreasing Cu-N-C bond angle (θ) with increasing Cu-NC bond distance (d). Lower: trend of increasing cyanide stretching frequency (ν_{CN}) with decreasing Cu-NC bond distance and increasing Cu-N-C bond angle. The two points for 9 in the upper plot arise from two crystallographically independent molecules.²² The two ν_{CN} values for 18 (2168, 2159 cm⁻¹) have been averaged in the lower plot. Without implication that the trends are necessarily linear, the data have been fitted by a least-squares method to the following equations: $\theta = -66.88d + 300.3$ ($r = 0.9646$); $d = -0.008191\nu_{\text{CN}} + 19.74$ ($r = 0.9545$); $\theta = 0.5650\nu_{\text{CN}} - 1057$ ($r = 0.9496$).

the presence of a slight excess of pyridine afforded by ¹H NMR analysis the Fe-CN-Cu product.

[Fe^{III}-CN-Cu^{II}] Bridge Structure Summary. The entire set of bridged assemblies 9-16 and 18 spans the Cu-N-C angle range 174(1)-139.8(9)° and the Cu-NC bond length interval 1.88(1)-2.45(1) Å, and encompasses four stereochemical arrangements at the Cu(II) site: TBP-axial (9, 18), d-SP-equatorial (10-12), SP-axial (13-15), and TO (16). The plot in Figure 9 (upper) demonstrates an essentially monotonic trend of decreasing bond length with increasing bond angle. This situation provides a previously unavailable opportunity to investigate the dependence of certain electronic features on bridge structure. Here we examine cyanide stretching frequencies, considerably augmenting our earlier database.²²

Cyanide Stretching Frequencies. When cyanide is incorporated in an M-CN terminal unit, the ν_{CN} value exceeds that of free or weakly bound cyanide because electron density is reduced in its sp σ^* MO. The formation of doubly bridged M-CN-M' is expected to increase the frequency farther provided the bridge geometry remains largely unchanged. A frequency decrease occurs when cyanide functions as a π -acid, owing to addition of electron density to the empty p π^* MOs.^{38,39}

(a) Synthetic Bridged Assemblies. Values of ν_{CN} for seven monobridged and two dibridged [Fe^{III}-CN-Cu^{II}] assemblies

(38) Shriver, D. F. *Struct. Bonding (Berlin)* **1966**, *1*, 32.

Table 6. Cyanide Stretching Frequencies

group	compound	ν_{CN} , cm^{-1}	
		solid ^d	CH ₂ Cl ₂ soln
CN ⁻	NaCN	2080 ^b	
Fe ^{III} -CN	1	2129	
Fe ^{III} -CN-Cu ^{II}	[9](ClO ₄) ₂	2177 ^c	2175
	[10](CF ₃ SO ₃)	2181 ^c	2177
	[11](ClO ₄) ₂	2175	2176
	[12](CF ₃ SO ₃)	2160	2164
	[13](PF ₆) ₂	2141	2143
	[14](ClO ₄)	2145	2153
	[15](ClO ₄) ₂	2151	
	ox. CcO (bovine heart) ^d		2151, ^e 2152 ^f
	ox. cytochrome <i>bo</i> (<i>E. coli</i>) ^d		2146 ^g
Fe ^{III} -CN-Cu ^{II} -NC-Fe ^{III}	[16](SbF ₆) ₂	2120	2121
Cu ^{II} -NC-Fe ^{III} -CN-Cu ^{II}	[18](ClO ₄) ₃	2168, 2159 ^c	2159
Fe ^{III} -NC-Cu ^I	[17](ClO ₄)	2100	2082

^a Mulls in Paratone-N oil. ^b Reference 39. ^c Reference 22. ^d Aqueous buffer solutions. ^e Reference 9. ^f Reference 12. ^g Reference 14.

in the solid state and in dichloromethane solution together with related data are presented in Table 6. The frequencies range from 2177 to 2120 cm^{-1} in the solid state; the range in solution is practically identical. All values except for **16** are higher than those of precursor heme complex **1**. Confirmation that these features are cyanide stretches was obtained by isotope substitution of one assembly. Incorporation of ¹³C¹⁴N⁻ and ¹²C¹⁵N⁻ into [(1-MeIm)Fe-CN-Cu(Me₆tren)]²⁺²² afforded $\nu_{\text{CN}} = 2138$ and 2150 cm^{-1} respectively, in the solid state compared to 2177 cm^{-1} for the unsubstituted compound. Values calculated from a simple harmonic oscillator model are 2137 and 2149 cm^{-1} , respectively. Note that, for the significantly bent bridges in **12**–**14** and **16**, the solution ν_{CN} values are within 10 cm^{-1} of those in crystals, strongly implying that nonlinear structures are retained in solution. The observed values are considerably higher than $\nu_{\text{CN}} = 2100 \text{ cm}^{-1}$ for **17**, where back-bonding in the bridge fragment Cu^I-CN has substantially reduced the frequency.

In Figure 9 (lower), the data reveal the trends of increasing cyanide stretching frequency with decreasing Cu-NC bond length and increasing Cu-N-C bond angle. Except for **10**, the trends are monotonic. From these data, we cannot discern whatever inherent effects the different Cu(II) ligands have on ν_{CN} values. We expect that these are small and are dominated by the local Cu(II) electronic and bridge geometric factors that are set by the local stereochemistry imposed by the ligands and their interactions with OEP. From the data available, the lowest stretching frequencies are associated with the SP-ax and TO stereochemistries. The situation is most simply viewed in terms of the bridge limiting electronic depictions **19** and **20**. As the bridge deviates from linearity and cyanide triple bonding in **19**, the contribution from **20** increases in the presence of a π -donor atom such as low-spin Fe(III). While it cannot be assured that **20** will induce a longer Cu-N bond, that is the case in the present set of compounds. Certainly a decrease in the Cu-N-C angle is expected to decrease the triple-bond character of bridging cyanide, as observed.



(b) **Enzymes.** Data for oxidized bovine heart cytochrome *c* oxidase (CcO) and a quinol oxidase from *E. coli* (Table 6) define the narrow range 2152 – 2146 cm^{-1} for these cyanide-inhibited enzymes; no other data for oxidized enzymes have been reported. In applying our database in Table 6 to the problem

(39) Nakamoto, K. *Infrared and Raman Spectra of Inorganic and Coordination Compounds*, 4th ed.; Wiley-Interscience: New York, 1986; pp 272–280.

of the structure of the oxidized binuclear site in cyanide-inhibited enzymes, we are cognizant of several limitations: (a) all reasonable geometries at the Cu(II) site have not been achieved;⁴⁰ (b) this site lacks the imidazole ligation of Cu_B and thus any inherent effects these ligands might have on ν_{CN} ; (c) the media in which synthetic species and enzymes have been measured are different.⁴¹ Nonetheless, because limitations b and c are expected to be minor effects, the database encompasses the enzyme frequencies with compounds of *established structures*, and structural parameters and frequencies correlate (Figure 9), we offer certain observations.

Our data establish that bands in the enzyme region can be achieved by possibility (i) noted at the outset, i.e., by a tight, somewhat bent [Fe^{III}-CN-Cu^{II}] bridge. This conclusion is at variance with a previous proposal that the 2151 cm^{-1} feature of bovine heart CcO was inconsistent with bridge bonding; instead, cyanide was thought to be bound to Cu_B.⁹ Thereafter, Caughey et al.¹¹ established that one cyanide is bound to the oxidized binuclear site and interpreted the collective evidence as favoring the formulation [Fe^{III}-CN-HImCu^{II}]; this appears to be equivalent to possibility (iii) observed earlier. While we cannot discount this formulation, our data indicate that it is not obligatory to reaching near-coincidence with the enzyme data. The best frequency matches occur when the Cu(II) site has SP-ax stereochemistry, a Cu-N bond distance in the 2.1 – 2.2 \AA region, and a Cu-N-C bond angle in the ca. 150 – 160° interval. At a longer distance or sharper angle, exemplified with **16**, the stretching frequency drops below the enzyme region.

In related work, we have established by magnetization and Mössbauer spectroscopy that the Fe(III) and Cu(II) spins are ferromagnetically coupled to afford a triplet ($S = 1$) ground state, and that the quadrupole splitting of Fe(III) is very similar to that in **9**.^{21,42} This mode of coupling and ground state are encountered in the oxidized enzymes.^{16,17} On the basis of the convergence of vibrational frequencies and electronic properties, we consider the [Fe^{III}-CN-Cu^{II}] bridge in the enzymes to be established.⁴³ Within the limits of the database, we would approximate its structure in terms of a linear Fe-CN fragment and the preceding range of parameters for the Cu-NC fragment.

Lastly, while our current work applies only to fully oxidized bridges, we note that formulations of one-electron-reduced bridges should be considered in terms of the structure of **17**. For example, in the bovine heart enzyme ν_{CN} features at 2131

(40) The most evident omissions are planar four-coordinate and TBP-eq. The two other possibilities based on five-coordination, SP-eq and SP-ax, are considered to be included.

(41) In one experiment, addition of 24 equiv of water to a nitromethane solution of **9** did not change ν_{CN} (2179 cm^{-1} in the pure solvent).²²

(42) Kauffmann, K.; Bominaar, E.; Lee, S. C.; Scott, M. J.; Day, E. P.; Holm, R. H.; Münck, E. Results to be published.

and 2090 cm⁻¹ have been attributed to [Fe^{III}-CN-HImCu^I] and [Fe^{III}-CN-ImCu^I] bridges.¹¹ Given $\nu_{\text{CN}} = 2100 \text{ cm}^{-1}$ for **17**, the possibility of a [Fe^{III}-NC-Cu^I] bridge, for which there has been no earlier precedent, should now be entertained even though Fe(III) in **17** is high-spin. Because Fe(III) remains low-spin in the enzyme, such an interpretation would appear to require this state with imidazole and N-bound cyanide axial ligation. No such native or synthetic heme with this ligation pattern appears to have been characterized, and the effect of a

(43) We note that ν_{CN} values of terminal Cu^{II}-CN groups can closely approach or overlap the enzyme range; e.g., the frequencies of [Cu(Me₆tren)(CN)](ClO₄),²² [Cu(tren)(CN)](BPh₄),⁴⁴ and [Cu(phen)₂(CN)](NO₃)₂·H₂O⁴⁵ (2140–2136 cm⁻¹) are just below the enzyme values. It appears most unlikely that cyanide would bind terminally to Cu(II) in the presence of Fe(III). The observation that [Cu(Me₆tren)(CN)]⁺ and [Fe(OEP)(OCIO₃)] yield **9**²¹ is one indication of the preference of C-bound cyanide for Fe(III). Exchange coupling between Fe(III) and Cu(II) at distances of ca. 5 Å require propagation via a covalent bridge. For these reasons we do not favor a binuclear enzymatic site in which the primary interaction is formation of the Cu^{II}-CN unit.

(44) Duggan, D. M.; Jungst, R. G.; Mann, K. R.; Stucky, G. D.; Hendrickson, D. N. *J. Am. Chem. Soc.* **1974**, *96*, 3443.

(45) Wicholas, M.; Wolford, T. *Inorg. Chem.* **1974**, *13*, 316.

high-spin/low-spin conversion on ν_{CN} in a [Fe^{III}-NC-Cu^I] (or [Fe^{III}-CN-Cu^I]) bridge is unknown. These are further matters for investigation in biologically relevant cyanide-bridged iron-copper assemblies.

Acknowledgment. This research was supported by NSF Grant CHE 92-08387. X-ray diffraction equipment was obtained by NIH Grant 1 S10 RR 02247. We thank Dr. S. C. Lee for useful discussions and Professor Y. Kishi for use of an infrared spectrophotometer.

Supplementary Material Available: X-ray structural information for the compounds in Tables 1 and 2 and tables of crystal and intensity collection data, positional and thermal parameters, interatomic distances and angles (78 pages); structure factor tables (293 pages). This material is contained in many libraries on microfiche, immediately follows this article in the microfilm version of the journal, and can be ordered from the ACS; see any current masthead page for ordering information.